Raman Scattering Studies of the High-Pressure Stability of Pentaerythritol Tetranitrate, $C(CH_2ONO_2)_4$

Kristina E. Lipinska-Kalita, Michael G. Pravica, and Malcolm Nicol*

High Pressure Science and Engineering Center, Department of Physics, University of Nevada Las Vegas, Las Vegas, Nevada 89154-4002

Received: May 23, 2005; In Final Form: August 10, 2005

High-pressure Raman scattering studies have been performed on a crystalline energetic material, pentaerythritol tetranitrate $C(CH_2ONO_2)_4$ (PETN), an important secondary explosive. In situ, ambient-temperature investigations employed diamond anvil cell techniques and nitrogen as a quasi-hydrostatic-pressure-transmitting medium. The pressure-induced alterations in the profiles of the Raman lines, including positions, bandwidths, and intensities, were studied in a compression sequence up to about 31.3 GPa and in a subsequent decompression to ambient conditions. The observed changes of the Raman spectra implied that PETN gradually densified and compressed smoothly up to the highest investigated pressures. Compression below 12 GPa gradually shifted all Raman peaks to higher frequencies without significantly changing their relative intensities or bandwidths. At higher pressures, the peak intensities of the Raman spectra decreased considerably and the bands broadened significantly. The Raman spectrum of the material quenched from 31.3 GPa to ambient conditions indicated that no pressure-driven permanent reconstructive modification or decomposition of the PETN structure occurred. That is, the spectral changes were completely reversible upon compression and subsequent decompression to ambient conditions.

Introduction

Pentaerythritol tetranitrate, $C(CH_2ONO_2)_4$ (PETN), is a well-known crystalline energetic material. In the past decade, numerous studies have aimed to understand the structural, electronic, mechanical, thermal expansion, vibrational, and elastic properties of PETN as well as to estimate the effects of compression on the structure of this material.[1−7] In particular, the observed anisotropy in the shock sensitivity of solid PETN has been the subject of much research interest.[8−11] Quantum mechanical calculations on the shock wave impact for PETN have sought to explain the chemical mechanism and the observed anisotropy of shock wave initiation.[12] Theoretical studies of hydrostatic compression, based upon the rigid-molecule approximation, calculated linear compressibilities of PETN crystals[4] which agree reasonably with experimental values to about 5 GPa. However, significant discrepancies occur at higher pressures. From experimental high-pressure studies of PETN by X-ray diffraction or neutron scattering at pressures to 4.3 and 10.5 GPa, respectively, linear and volumetric hydrostatic compressions have been estimated; however, the results of these studies are inconsistent.[13,14] They show discrepancies in the linear or volumetric compressions which increase at higher pressures. Despite considerable theoretical and experimental efforts aimed at evaluating the effects of compression on the structure of the PETN, detailed experimental data are still lacking, particularly at high pressures.

A comprehensive understanding of the properties of PETN, especially at high pressures, is of great importance for applied chemistry and materials science as well as for various future practical applications of this material. In our recent high-pressure synchrotron radiation X-ray diffraction studies of neat PETN, we discovered the onset of a low-to-high-density phase transition at about 8 GPa. We postulated that the crystal lattice partly transforms from its tetragonal ambient-pressure structure to an orthorhombic high-pressure structure.[15−17]

The results presented here expand in depth on our previous X-ray diffraction study and are part of a research program aimed at extending the current understanding of pressure-driven structural transformations of PETN by employing a multitechnique approach. We performed in situ high-pressure Raman scattering studies of PETN in compression from ambient pressure to 31.3 GPa and subsequent decompression to ambient pressure. A goal of this study was to follow possible pressure-induced structural transformations in PETN. In particular, we hoped to confirm the previously reported low-to-high-density phase transition.[15−17]

Raman scattering data of PETN in the literature have been obtained at ambient pressure primarily to increase the detection limit for this compound in different media. The main goals of such studies were to demonstrate the potential of Raman spectroscopy as a rapid, highly selective screening methodology for detecting trace levels of a range of explosives, including PETN.[18−23]

Experimental Section

Submicrometer, polycrystalline PETN was obtained from Los Alamos National Laboratory. For in situ Raman scattering studies, polycrystalline PETN was compressed in a Mao-Bell-type diamond anvil cell (DAC). A rhenium gasket was preindented to 45 μm and placed between two diamonds each with 300 μm diameter cutlets. The sample chamber consisted of a 90 μm diameter hole, drilled via electric discharge machining, in the preindented gasket. A 5 μm grain of ruby crystal was loaded into the sample chamber for determining pressure

* To whom correspondence should be addressed. Phone: (702) 895-1725. E-mail: nicol@physics.unlv.edu.

10.1021/jp052713f CCC: $30.25
Published on Web 09/24/2005

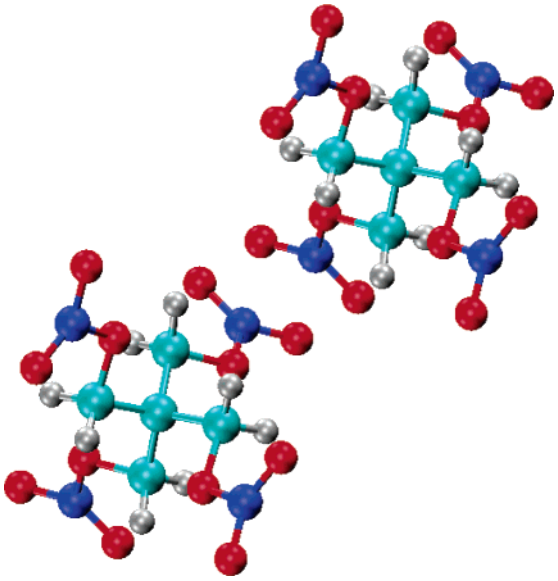

Figure 1. A ball-and stick model for two PETN molecules (sketch courtesy of E. Kim and P. Weck). Atoms: green, carbon; red, oxygen; blue, nitrogen; white, hydrogen.

together with liquid nitrogen to provide quasi-hydrostatic conditions. After each pressure change, we waited about 10 min before subsequently measuring the Raman spectra to allow the PETN, the gasket, and nitrogen to relax to the new conditions.

Room-temperature Raman scattering spectra were collected during a compression and decompression sequence. The pressure was increased gradually from 1.6 GPa, the first pressure after loading with liquid nitrogen, to 31.3 GPa and subsequently decreased to ambient conditions. The 514.5 nm line of an argon ion laser with a power of 100 mW at the sample surface provided the Raman excitation. The scattered light was collected in backscattering geometry, and focused onto the entrance slit of a double monochromator (Jobin-Yvon model U1000) coupled to a liquid-N_2-cooled CCD (Jobin-Yvon) detector.

Results and Discussion

The purity of the PETN sample used in this experiment was checked by powder X-ray diffraction, followed by Rietveld refinement of the structure, and then Raman scattering spectroscopy.

In the crystalline phase and at ambient pressure, the PETN molecule has 29 atoms and S_4 symmetry; the unit cell of the solid contains two molecules (Figure 1). The 81 internal vibrational modes of a PETN molecule (Γg) belong to the following irreducible representations of the S_4 molecular point group: $\Gamma g = 20A + 21B + 20E$, and all modes are Raman active.[26,27] The Raman mode assignment is based on theoretical calculations of normal-mode frequencies and determined mode symmetries performed for a single molecule by Gruzdkov et al.[28]

It is noteworthy that that the calculated and measured vibrational spectra agree very well since the theoretical calculations[28] were performed for a single PETN molecule, while the experimental data were obtained for crystalline PETN. Therefore, the PETN molecule does not appear to be appreciably distorted by the crystal field, and factor group splittings are small.

As previously mentioned, nitrogen was used in this experiment as a chemically inert, quasi-hydrostatic-pressure-transmitting medium. Figure 2 shows Raman scattering spectra of the nitrogen vibrons collected during compression to 31.3 GPa and subsequent decompression to ambient pressure.

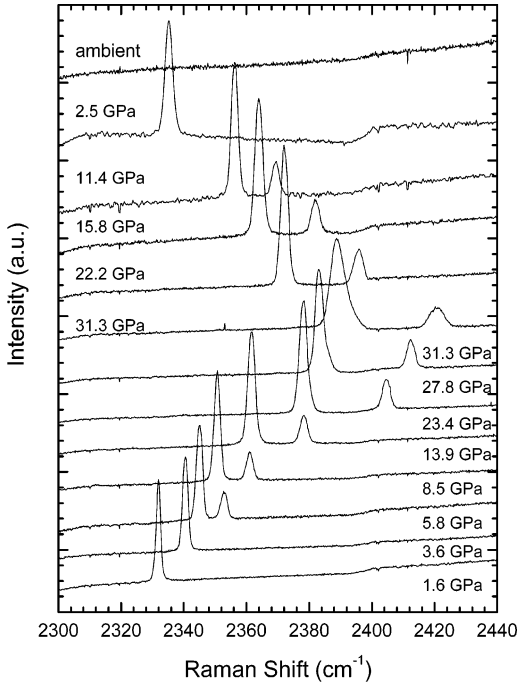

Figure 2. Raman scattering spectra showing the vibrational frequency shifts of the nitrogen vibrons, in compression from 1.6 to 31.3 GPa, and in the following decompression sequence down to ambient pressure.

In nitrate esters such as PETN, each NO_2 group bonds through an oxygen atom to a tetrahedral carbon atom (Figure 1). The typical vibrational spectrum of such a structure consists of intense broad bands at about 870−890 cm^{-1} and assigned to NO stretching modes, symmetric and asymmetric stretching vibrations of the nitro groups at approximately 1280−1300 and 1630−1670 cm^{-1}, respectively, as well as CH stretching modes at about 3000 cm^{-1}.[22]

Raman spectra measured in a compression sequence from 1.6 to 10.3 GPa and from 10.3 GPa to the highest pressure of our experiment, 31.3 GPa, are shown in parts a and b, respectively, of Figure 3. All spectra exhibited increased background scattering at wavenumbers above 1200 cm^{-1} because of the strong Raman scattering from diamonds. Lattice modes of nitrogen are noticeable as low-frequency weak bands in Figure 3 and are in good agreement with those reported by Bini et al.[30] At pressures between 15.6 and 20.1 GPa, changes of the nitrogen lattice modes are attributed to the δ (cubic) to ϵ (rhombohedral) phase transition in solid nitrogen. Another new lattice mode emerges at 26 GPa because of the transition from the ϵ phase to a second rhombohedral ζ phase.

The Raman spectra of PETN in compression below 12 GPa (Figure 3) consist of several sharp peaks with narrow bandwidths. The dominant features at low wavenumbers are symmetric, narrow peaks centered on 600 cm^{-1} which primarily correspond to vibrations involving carbon atoms (see Table 1). In particular, strong peaks located at 548, 595, and 630 cm^{-1} are assigned to C_5 skeletal, CC bending, and CCC deformation modes, respectively. The intense peaks at 850 and 882 cm^{-1} are attributed to CC and NO stretching modes, respectively. Finally, the peaks at 1047 and 1253 cm^{-1} are assigned to CC and CH bending modes. A detailed assignment of all observed Raman peaks based on recently reported theoretical calculations[28] is presented in Table 1.

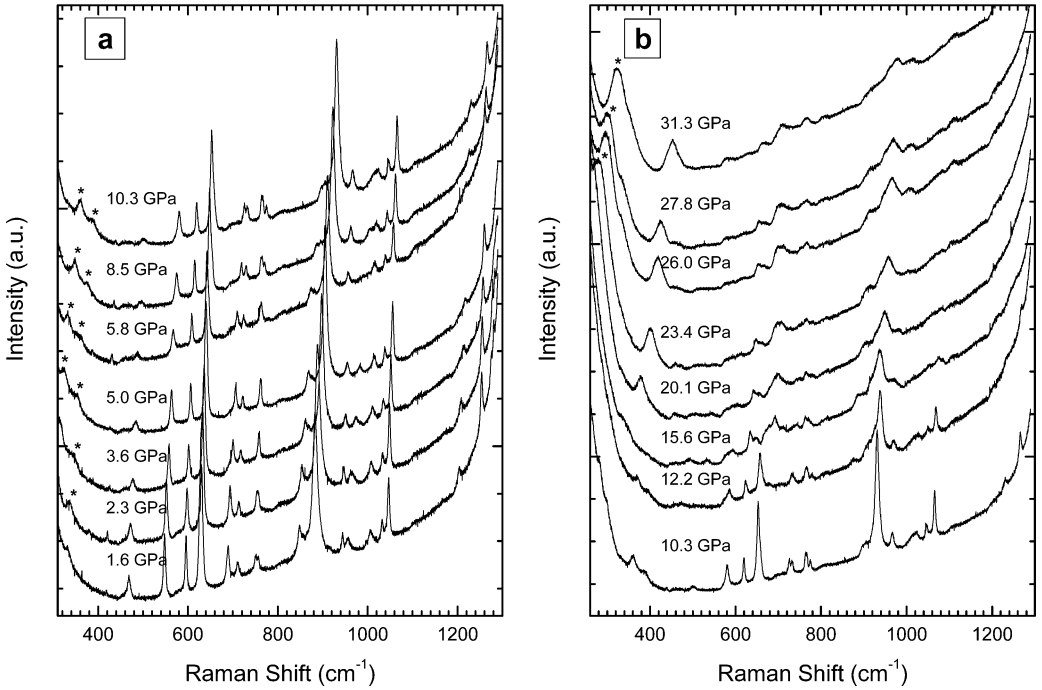

Figure 3. In situ (DAC) Raman scattering spectra of PETN collected in a compression sequence from 1.6 to 31.3 GPa. The bands near 300 cm^{-1} denoted with asterisks derive from nitrogen lattice modes.

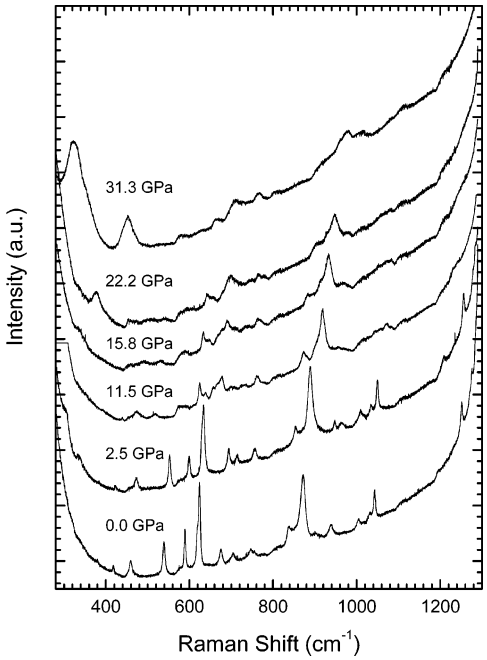

Figure 4. In situ Raman scattering spectra of PETN collected in the decompression sequence from the highest investigated pressure, 31.3 GPa, to ambient conditions.

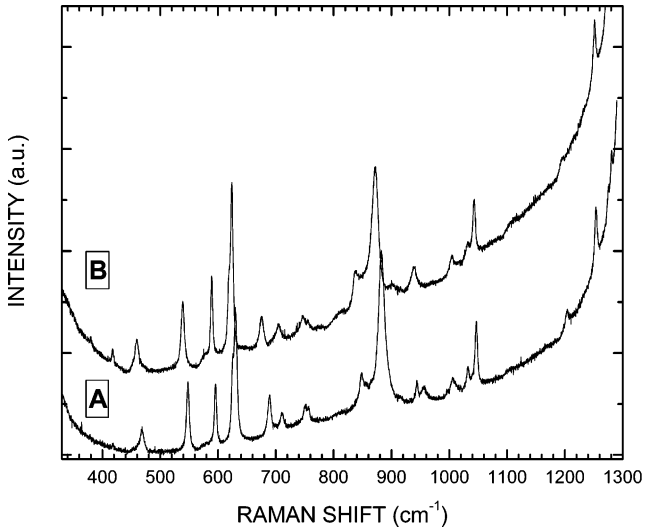

Figure 5. Comparison of the Raman scattering spectra: (A) 1.6 GPa at the beginning of the compression sequence; (B) sample decompressed from 31.3 GPa to ambient pressure.

As shown in Figure 3, as pressure increases, all Raman peaks gradually shift toward higher frequencies. Furthermore, upon compression to about 10.3 GPa the spectral profiles, bandwidths, and relative intensities are almost unchanged. In particular, no changes characteristic of a possible phase transition in PETN occur between 6 and 11 GPa. With successive pressure increases to 12.2 GPa and above, the Raman peaks decrease remarkably in peak intensity and their spectral profiles broaden inhomogeneously, which we attribute to increasingly nonhydrostatic conditions. At increasingly higher pressures, the spectra become more and more diffuse so that, at and above 15.6 GPa, only the strongest bands centered around 650−700 and 950 cm^{-1} are clearly evident. Only a few very broad bands can be detected at the highest pressure of this experiment, 31 GPa (see also Figure 6). We attribute the pressure-induced modifications of the profiles of the Raman peaks in Figure 3, the shifts to higher wavenumbers, the absence of changes in the peak intensities below 10 GPa, and significant increases of the bandwidths above this pressure to a continuous densification of PETN in an increasingly nonhydrostatic environment.

Decompression studies were performed to test whether the spectral changes observed in compression are reversible. Figure 4 shows Raman scattering spectra of the PETN quenched gradually from 31.3 GPa to ambient conditions. At first, all peaks remained broad as the pressure was released. However, below 11.5 GPa, the peak intensities increased, and the frequency shifts resembled those seen at comparable pressures during compression.

In Figure 5, we compare the Raman scattering spectrum measured at the beginning of compression at 1.6 GPa and that

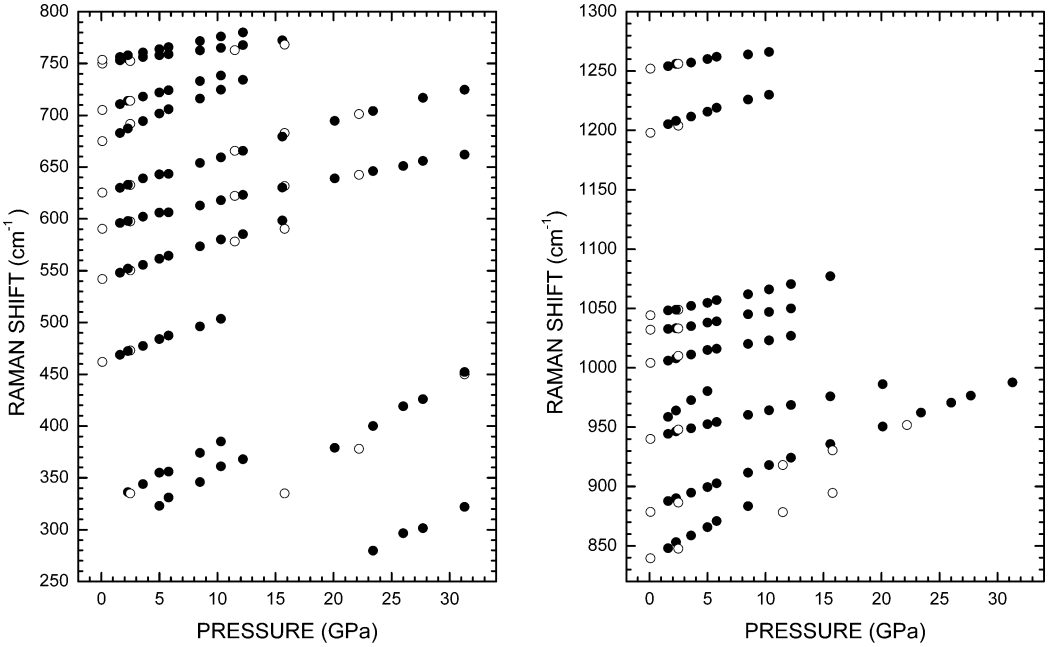

Figure 6. Pressure-driven frequency shifts of PETN Raman scattering peaks in compression (solid circles) and decompression (open circles) sequences between ambient pressure and 31.3 GPa. The positions of all peaks gradually shift with increasing pressure toward higher energies. These data are only for peaks whose positions were clearly identified.

of the sample decompressed to ambient pressure. The two spectra are nearly indistinguishable except that the peaks return to positions with slightly lower frequencies than those observed at the beginning of compression (1.6 GPa). On the whole, the alterations of Raman spectral profiles observed in compression and in decompression sequences indicate that any pressure-induced, local structural rearrangements in the PETN crystal are fully reversible.

The pressure dependence of the Raman peak positions in compression and decompression sequences is shown in Figure 6. Compression shifts the peak positions almost linearly to higher wavenumbers, and these changes are fully reversible on decompression. Above 12 GPa, pressure-induced broadening and decreasing intensities made it difficult to determine some peak positions precisely. Thus, we include in Figure 6 only data for the peaks that we could clearly discern.

Finally, the Raman peaks due to the symmetric and antisymmetric stretching vibrations of CH_2 units (see Table 1) were observed between 3000 and 3100 cm^{-1}. The two peaks located at 3019 and 3068 cm^{-1} at the beginning of the compression sequence (1.6 GPa) were detected only up to about 8.5 GPa. They reappeared at the expected, slightly lower frequencies (3008 and 3056 cm^{-1}) in the Raman spectrum of PETN decompressed to ambient conditions.

Because of the low molecular and crystal symmetries, very few normal modes uniquely represent motions of specific functional groups of the PETN molecules. In all the frequency ranges studied, the ambient pressure mode frequencies observed in our study closely agreed with the frequencies calculated for the free PETN molecule, and with the mode frequencies reported for bulk PETN.[28] This implies that the Davydov splittings are small and the crystal field does not strongly perturb the PETN molecule.

In situ (DAC) high-pressure Raman studies illustrate that compression of PETN in a nitrogen medium to 31.3 GPa is elastic and relaxes immediately after pressure release. The Raman spectra did not indicate any reconstructive structural changes. In our recent synchrotron radiation X-ray diffraction studies of neat PETN, we reported the onset of a low-to-high-

TABLE 1: Experimental and Calculated Frequencies[28] of Raman Modes of PETN[a]

	exptl freq, this work (cm^{-1})					
no.	1.6 GPa	0 GPa	exptl freq[28] (cm^{-1})	calcd freq[28] (cm^{-1})	irr rep	assignment[28]
1	468.7 w	459.7 w	459 m	453	E	CCC def, O′N str, NO_2 r
2	548 m	539 m	539 w	536	B	C_5 skl, CH_2 w, O′N str
3	595.2 m	588.7 m	589 s	585	A	CC b, ONO_2 r
4	625.7 sh	619.7 sh	619 sh	617	B	C_5 skl, ONO_2 r
5	630.3 s	623.4 s	624 s	623	E	CCC def, ONO_2 r
6	689.3 m	676 w	676 m	673	A	O′N str, CC str, NO_2 sc
7	711.5 w	704.6 w	704 m	710	E	O′N str, CCC def, NO_2 r
8	752.2 w	747 w	746 w	753	B	CCC def, O′N str
9	756.5 sh	755.5 sh	755 w	760	B	ONO_2 umb, CCC def
10	848.9 m	839 m	839 m	842	A	CC str
11	881.8 s	872.3 s	873 s	886	A	O′N str, CC str
12	911.5 sh	901.3 sh	900 sh	934	B	CCC def, CH_2 r
13	944.7 w	939.5 w	939 w	952	E	CH_2 t, CCC def
14	956.6 w		995 sh	1023	A	CH_2 r, CO st
15	1006 w	1004.3 w	1004 w	1038	E	CO st, CCC def
16	1031.8 w	1032.2 w	1037 sh	1074	B	CO st, C_5 skl, NO_2 r
17	1047 m	1043.3 m	1044 m	1071	A	CH_2 t, CC b
18	1204 w	1196.3 w	1195 m	1212	E	CCC def, CH_2 wag
19	1253.7 s	1251.4 s	1253 s	1274	A	CH b
20	3019 s	3008 s	2987 vs	3105	A	CH_2 str (s)
21	3068 s	3056 s	3025 s	3161	E	CH_2 str (as)

[a] This table includes mode frequencies originated from our experimental spectra at the beginning of the compression sequence (1.6 GPa) and at the end of the decompression sequence and theoretically calculated mode frequencies and experimental data for bulk PETN at ambient pressure from the literature.[28] Intensity and mode assignments:[26,27] vw, very weak; w, weak; m, medium; s, strong; vs, very strong; sh, shoulder; st, stretch (for the CC st, the quaternary carbon is stationary, and only the secondary carbons vibrate); b, bend; sc, scissors (in-plane symmetric bending modes); r, rock (in-plane vibrations of three or more atoms of a planar group); umb, umbrella (the ONO_2 umbrella motion, an out-of-plane vibration of the nitrogen accompanied by the counter phase motion of the oxygens); wag, wagging (out-of-plane modes); skl, skeletal (for the C_5 skl, vibrational amplitudes of all five carbons are comparable); t, torsion; def, deformation (for the CCC def, the motion of the quaternary carbon atom is large and relatively the secondary carbon atoms move only slightly); a, antisymmetric; s, symmetric; O′, the ester oxygen.

density phase transition near 8 GPa.[15−17] As can be seen from Figures 3 and 4, however, the increase of pressure from ambient to 10.3 GPa does not provide evidence of the prior-mentioned phase transition. The line broadening at higher pressures may well be due to inhomogeneous effects of increasing but weak nonhydrostatic stresses in the nitrogen. This can be tested in future experiments with better quasi-hydrostatic media such as helium or hydrogen. The differences between the two aforementioned experiments are not unexpected, as the X-ray diffraction study was performed on neat PETN without a pressure-transmitting medium, that is, under more severe nonhydrostatic conditions than in this experiment. The liquid and solid nitrogen used to transmit pressure to the PETN in these experiments provided quasi-hydrostatic conditions, at least to 12 GPa.[29] By comparing the X-ray diffraction and Raman scattering experiments, we conclude that the absence of a pressure-transmitting medium created a favorable environment that initiated the low-to-high-density phase transition. More precisely, we suspect that shear stresses and shear deformations are the driving forces which create defects where the transition at intermediate high pressures may commence.

Conclusions

We performed in situ, diamond anvil cell, Raman scattering studies of PETN during compression and subsequent decompression cycles to 31 GPa. The principal aim of this experiment was to identify any pressure-induced structural transformations, including possible phase transitions. The observed Raman spectral changes imply that PETN compresses elastically up to 31.3 GPa and that the structure of the pressure-quenched material is identical to that of the starting material. We interpret the persistence of three vibrational modes over the entire investigated pressure range and the demonstrated reversibility of the Raman spectral changes in terms of intrinsic high flexibility of the structure of this organic molecule as well as the entire molecular crystal. In the pressure range studied, we observed no new Raman peaks which could provide direct evidence of a pressure-induced phase transformation. This observation is different from that of our previous X-ray diffraction studies where the beginning of a phase transition was reported at about 8 GPa.[15−17] However, we believe that the observed pressure-driven variations of the X-ray diffraction patterns demonstrating a phase transition are strongly influenced by the nonhydrostatic conditions of the X-ray experiments and that the transition is shear-driven. In future work, we will endeavor to elucidate the potential contribution of anisotropic stresses in initiating phase transitions in energetic materials by extending our spectroscopy and X-ray diffraction studies with different pressure-transmitting media and extended pressure ranges.

Acknowledgment. We thank David S. Moore for supplying the PETN samples and Hubertus Giefers for assistance with nitrogen loading. We acknowledge support from the U.S. Department of Energy Cooperative Agreement No. FC08-01NV14049 with the University of Nevada Las Vegas.

References and Notes

(1) Trotter, J. *Acta Crystallogr*. **1963**, *16*, 698.
(2) Kuklja, M. M.; Kunz, A. B. *J. Appl. Phys*. **2001**, *89*, 4962.
(3) Bunte, S. W.; Sun, H. *J. Phys. Chem. B* **2000**, *104*, 2477.
(4) Sorescu, D. C.; Rice, B. M.; Thompson, D. L. *J. Phys. Chem. B* **1999**, *103*, 6783.
(5) Gan, C. K.; Sewell, T. D.; Challacombe, M. *Phys. Rev. B* **2004**, *69*, 35116.
(6) Park, T.-R.; Dreger, Z. A.; Gupta, Y. M. *J. Phys. Chem. B* **2004**, *108*, 3174.
(7) Pastine, D. J.; Bernecker, R. R. *J. Appl. Phys*. **1974**, *45*, 4458.
(8) Dick, J. J. *Appl. Phys. Lett* **1984**, *44*, 859.
(9) Dick, J. J.; Mulford, R. N.; Spencer, W. J.; Pettit, D. R.; Garcia, E.; Shaw, D. C. *J. Appl. Phys*. **1991**, *70*, 3572.
(10) Yoo, C. S.; Holmes, N. C.; Souers, P. C.; Wu, C. J.; Ree, F. H.; Dick, J. J. *J. Appl. Phys*. **2000**, *88*, 70.
(11) Dick, J. J.; Ritchie, J. P. *J. Appl. Phys*. **1994**, *76*, 2726.
(12) Gruzdkov, J. A.; Gupta, Y. *J. Phys. Chem. A* **2000**, *104*, 1169.
(13) Ollinger, B.; Halleck, P. M.; Cady, H. H. *J. Chem. Phys*. **1975**, *62*, 4480.
(14) Dick, J. J.; von Dreele, R. B. *Shock Compression of Condensed Matter*; American Institute of Physics: Melville, NY, 1997.
(15) Lipinska-Kalita, K. E.; Pravica, M.; Nicol, M. To be submitted.
(16) Pravica, M.; Lipinska-Kalita, K. E.; Giefers, H.; Shen, Y-R.; Nicol, M.; Somayazulu, M.; Hu, M. *Bull. Am. Phys. Soc*. **2005**, *50* (1 B11 9), 164.
(17) Lipinska-Kalita, K. E.; Pravica, M.; Nicol, M. *Bull. Am. Phys. Soc*. **2005**, *50* (1 R1 215), 1035.
(18) Carver, F. W. S.; Sinclair, T. J. *J. Raman Spectrosc*. **1983**, *14*, 377.
(19) Carver, F. W. S.; Wyndham, D. P.; Sinclair, T. J. *J. Raman Spectrosc*. **1985**, *16*, 377.
(20) McNesby, K. L.; Wolfe, J. E.; Morris, J. B.; Pesce-Rodriguez, R. A. *J. Raman Spectrosc*. **1994**, *25*, 75.
(21) Fell, N. F.; Widder, J. M.; Medlin, S. V.; Morris, J. B.; Pesce-Rodriguez, R. A.; McNesby, K. L. *J. Raman Spectrosc*. **1998**, *27*, 97.
(22) Lewis, I. R.; Daniel, N. W., Jr.; Griffiths, P. R. *Appl. Spectrosc*. **1997**, *51*, 1854.
(23) Munro, C. H.; Pajcini, V.; Asher, S. *Appl. Spectrosc*. **2005**, *51*, 1722.
(24) Larson, A. C.; von Dreele, R. B. *GSAS Manual*; Report LAUR86-748; Los Alamos National Laboratory: Los Alamos, NM, 1988.
(25) Toby, B. H. EXPGUI, a graphical user interface to GSAS. *J. Appl. Crystallogr*. **2001**, *34*, 210.
(26) Cotton, F. A. *Chemical Applications of Group Theory*; Wiley: New York, 1990.
(27) Fateley, W. G.; Dollish, F. R.; McDevitt, N. T.; Bentley, F. F. *IR and Raman Selection Rules for Molecular Vibrations*; Wiley-Interscience: New York, 1972.
(28) Gruzdkov, Y. A.; Gupta, Y. M. *J. Phys. Chem. A* **2001**, *105*, 6197.
(29) Schmidt, S. C.; Schiferl, D.; Zinn, A. S.; Ragan, D. D.; Moore, D. S. *J. Appl. Phys*. **1991**, *69*, 2793.
(30) Bini, R.; Ulivi, L.; Kreutz, J.; Jodl, H. J. *J. Chem. Phys*. **2000**, *112*, 8522.